INTERNATIONAL JOURNAL OF PRECISION ENGINEERING AND MANUFACTURING Vol. 15, No. 10, pp. 2031-2039 OCTOBER 2014 / 2031
DOI: 10.1007/s12541-014-0560-1

Investigation on Machining Characteristic of Pneumatic Wheel based on Softness Consolidation Abrasives

Xi Zeng[1,#], Shi-ming Ji[1], Ming-sheng Jin[1], Da-peng Tan[1], Jue-hui Li[1], and Wen-tao Zeng[1]

1 Key Laboratory of Special Purpose Equipment and Advanced Manufacturing Technology, Zhejiang University of Technology, Hangzhou, China, 310014
Corresponding Author / E-mail: franckie@126.com, TEL: +86-138-5813-1148, FAX: 86-571-88320372

KEYWORDS: Softness consolidation abrasives, Laser hardening surface, Machining, High hardness

In order to improve material removal rate of laser hardening workpiece and also make machining tool suitable for free-form surface, a new method based on the softness consolidation abrasives (SCA) is put forward, which means the abrasives are consolidated on the outer layer of pneumatic wheel to achieve the softness-machining. Binder selecting test shows that acidic silicone is proved to suit for consolidating particles in cutting process. Combined with robot, the machining system has been established. The machining effects of SCA are investigated when it faces with workpiece of different hardness. According to the Preston predicted model, the simulation results of stress and velocity are proven by analysis of average roughness in the contact region. The contrastive machining experimental results show that SCA can supply high cutting stress for material removal and fit for freeform surface's machining by self-adjustment of flexible body.

Manuscript received: January 16, 2014 / Revised: May 15, 2014 / Accepted: June 4, 2014

NOMENCLATURE

SCA= softness consolidation abrasives

1 Introduction

The surface of mold hardened by the laser technology has especial advantages such as prolonging life of mold, hardening local area for reducing costs and making the freeform surface smooth in hardening process.[1,2] Suvi et al. reviews the use of laser in surface hardening and presents its outstanding performance.[3] Lamikiz et al. study the laser polishing of parts and Ukar et al. discuss parameters of selective laser sintering.[4,5] Their jobs indicate that laser can play an important role in local parts hardening of mold. Meantime, these merits bring lots of problems into the finishing process. Some researchers such as Yasumaru et al. and Yasa et al. claim that surface will become difficult-to-cut because of high hardness and wear resistance.[6,7] In addition, owing to the irregular free-form surface, manual process has been adopted as the main form of finishing methods, which consumes nearly 40% of processing time. These problems are far from being resolved with effectiveness and also lack in-depth study.[8,9]

The procedure of finishing can be described as the abrasives moving on the surface of workpiece repeatedly under the support of medium to achieve the material removal. So, the medium can be distinguished as rigid or flexible medium. The grinding method can be recognized as an important finishing method with rigid medium. However, restricted by the shape of the rigid wheel, it only can be used on the specific local area of freeform surface. It is difficult to directly obtain the mirror-grade surface. Abdalslam et al. have presented spherical grinding wheel for freeform surface.[10,11] But this kind of wheels always had small contact area with surface, which could not work with high-efficiency. The belt grinding method has also been proposed for irregular surface by Mezghani et al. and Huang et al.[12,13] But the two traction wheels supplying for power lack of self-profiling capability of belt wheel in any directions. In the case of flexible medium, magnetorheological jet polishing method is presented by Tricard et al. and soft abrasive flow polishing method is studied by Ji et al. for machining.[14,15] However, the particles do not have high material removal capacity enough in these situations. It is difficult to be effectively applied to the hard surface's finishing process.[16,17]

According to the literature above, it is found that there is still no tool which possesses both profiling capability and high material removal ability by now. In few of wide prospects of laser hardening mold,

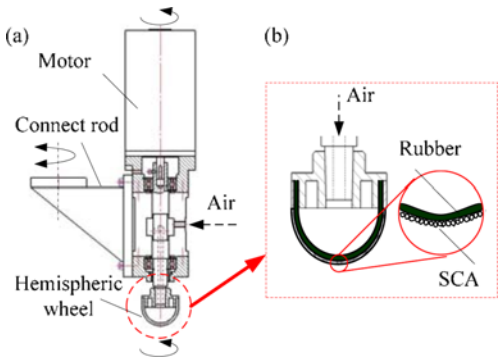

Fig. 1 The structure of SCA pneumatic wheel: (a) Overall structure, (b) Microstructure

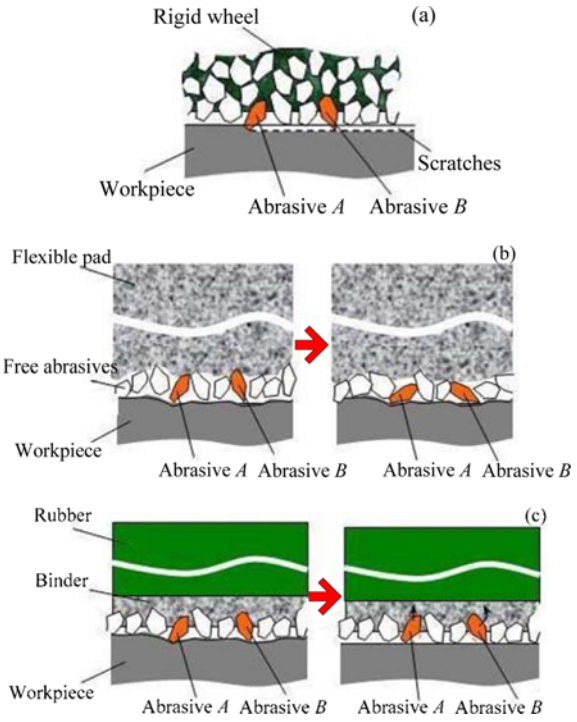

Fig. 2 Different movements of abrasives: (a) Fixed abrasives, (b) Free abrasives, (c) SCA

finishing technology is of great significance for the applications of the laser hardening technology in the industrial field of mold. In this study, a new method based on the softness consolidation abrasives is proposed for laser hardening freeform surface, whose characteristic is studied for improving efficiency and accuracy of machining.

2. Characteristic of SCA and Simulation

2.1 Design of SCA

SCA means that the abrasive particles are consolidated on the pneumatic wheel by the binder. The structure of SCA is shown in Fig. 1.

Pneumatic wheel is hollow hemisphere wheel which is constituted by the rubber. The surface of wheel is covered with a layer of abrasive by the polymer binder. The flexibility of hollow hemisphere wheel is adjusted by inner air pressure and its rotation is controlled by the inside motor. It can be easily used in conjunction with the robot by the connect rod for auto-finishing. Fig. 2 shows the different characteristics among fixed abrasives, free abrasives and SCA.

The plenty of the abrasives are consolidated on the surface by the polymer binder. As a result, in contrast to those free abrasives employed in the machining method, SCA can get more stable support from nearby polymer to obtain effective cutting. In this way, the movement of particles can be changed from rolling into sliding on the surface and its cutting ability is enhanced obviously. Opposed to the fixed abrasives on the rigid wheel, the pneumatic wheel is flexible enough to self-adapt to the changes of local curvature and to take large shape of copying contact between tools and workpiece. Meanwhile, its macro flexible performance would not bring damage into the surface. The outer layer of SCA ensures excellent elastic condition and dynamic constraint for each abrasive. It ensures the high-efficiency of machining as well as keeping deep-scratches away.

Table 1 Constants in the wheel

H_w	Wheel hardness	48 HA
D_w	Diameter of wheel	10 mm
δ_w	Thickness of wheel	2 mm
E_w	Elastic modulus	0.008 GPa
σ_w	Poisson's ratio	0.47
h	Indentation depth	2 mm
p_i	Inner air pressure	0.08 MPa

Table 2 Constants in the workpiece

μ	Friction coefficient	0.18
ρ_f	Density of workpiece	7.85 gcm^{-3}
E_f	Elastic modulus	156 GPa
σ_f	Poisson's ratio	0.29
σ_b	Yield stress	21.5 $KNcm^{-3}$
R_1	Radius of concave surface	60 mm
R_2	Radius of convex surface	60 mm
θ_1	Radian of concave surface	$\pi/6$
θ_2	Radian of convex surface	$\pi/6$

2.2 Simulation and results

2.2.1 Analysis of stress distribution

SCA and rubber can be recognized as an entirety of the wheel in the simulation. The constants in the wheel are shown in Table1.

The surfaces of workpiece are treated as flat surface, concave surface and convex surface respectively in accordance with the characteristic of freeform surface. The constants in the workpiece are shown in Table 2.

According to the parameters mentioned above, the contact models between SCA and freeform surface are established by ANSYS. The stress and strain are shown in Fig. 3.

On the basis of simulation, two conclusions are obtained: (1) Due to large contact between flexible body and rigid body, there is a good profiling for machining, especially for concave surface. It possesses strong adaptive ability to compensate for small contact and poor profiling of rigid wheel; (2) The distribution of stress has a direct bearing on feeding distance and it shows an irregular decreasing trend from the center to the periphery. The results show that the flexible wheel is fit for the freeform surface better than the rigid wheel.

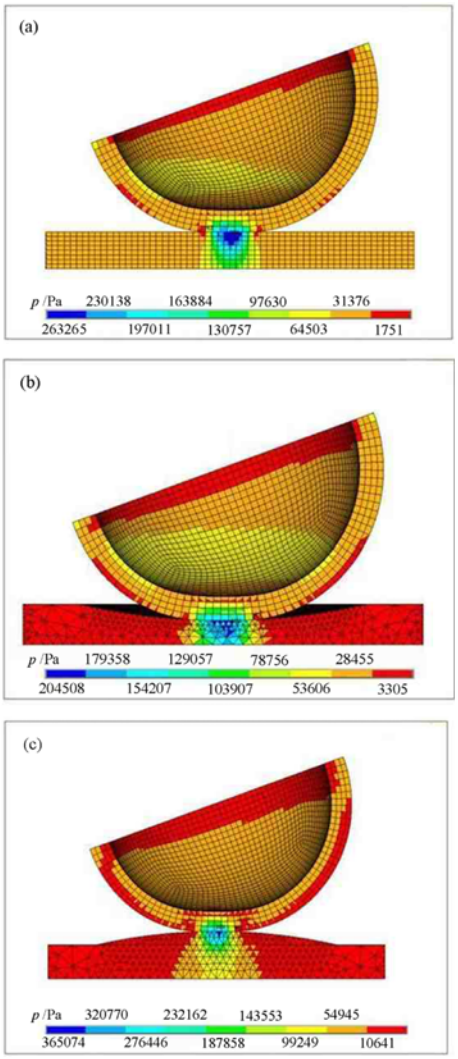

Fig. 3 Contact process simulations: (a) Contact with flat surface, (b) Contact with concave surface, (c) Contact with convex surface

However, the distribution of stress in the contact area shows irregular characteristic, which needs to be analyzed in detail.

2.2.2 Stress simulation in the contact area

It has been confirmed that the indentation depth has important relationship with the distribution of stress.[18] And then, the procedure of simulation is operated with different indentation depth. The results are shown in Fig. 4. Here, *s* means the contact area and *h* is set as 0.5 mm, 1.5 mm, 5 mm and 10 mm respectively.

It is found that the stress presents a trend of growth with feeding distance when *h* is in the range of 0.5 mm to 1.5 mm. In this case, the stress seems like controllable to be concentrated. However, it still has not been of optimal effect yet, which possesses few conditions for large-area contact for cutting. When *h* is from 1.5~5 mm, the stress diffuses from the center to the peripheral area. The wheel is of the maximum stress for the material removal and proper deformation for profile copying with the workpiece. When *h* is beyond the 5 mm, the shape of the wheel become uncontrollable and the stress is also deconcentrated. The simulation results provide a viable control solution for SCA machining method facing with the freeform surface with high hardness.

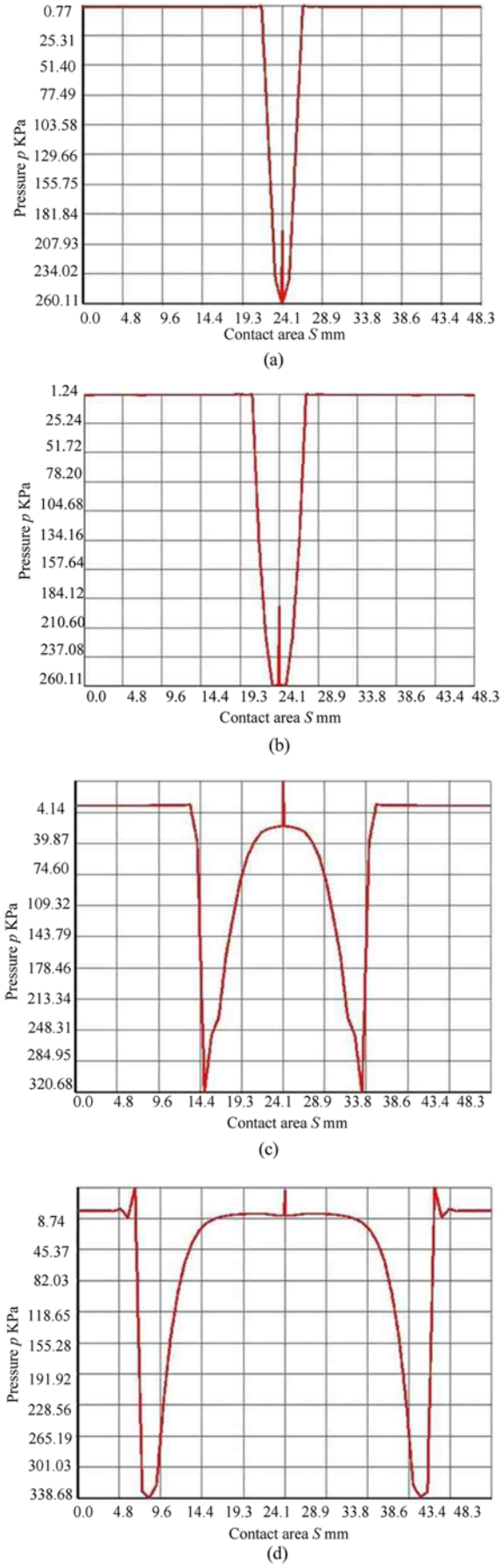

Fig. 4 Stress in the normal direction: (a) *h*= 0.5 mm, (b) *h*= 1.5 mm, (c) *h*= 5 mm, (d) *h*= 10 mm

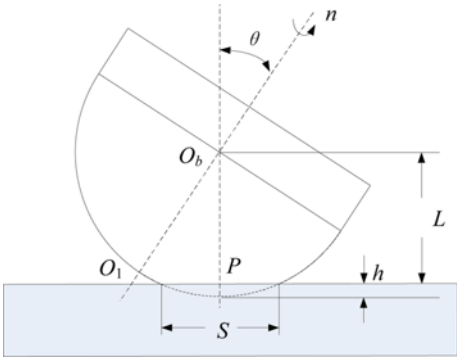

Fig. 5 Factors working on the rotation of wheel

Table 3 Parameters of simulation

n (r/min)	D_w (mm)	δ_w (mm)	θ (°)	h (mm)	p (MPa)
1600	40	2	20	2	0.08

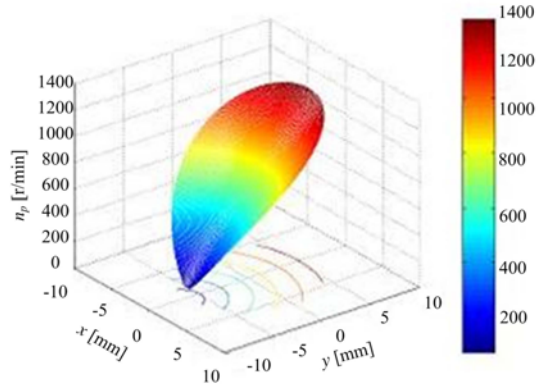

Fig. 6 Velocity of particle on the contact surface

2.2.3 Analysis of velocity distribution

Excluding the contact stress, the other vital factor related with material removal is velocity of the particles of SCA. As it mentioned above, the contact process leads to deformation of wheel. So, the factors about wheel as shown in Fig. 5 have important relationship with velocity of the particles. Where point O_b is the center of wheel, O_1 is the intersection between the central axis of the wheel and the surface of workpiece. L is the distance from O_b to the flat surface. θ is the inclination angle. n is the rotation velocity of wheel.

Choose O_1 as original zero and coordinate system is established, whose x axis is cast shadow of central axis of wheel on the contact surface and y axis goes through the O_1 and is perpendicular to x axis. The velocity of particle P on the contact surface can be deduced as Eq. (1). R is radius of wheel.

$$n_p(x,y) = n\sqrt{[(R-h)\sin\theta + x\cos\theta]^2 + y^2} \quad (1)$$

Under the parameters as Table 3, according to Eq. (1), the velocity of every particle on the contact surface can be presented as Fig. 6.

It is found that the contact area presents oval shape. The velocity increases with the growth of x value and shows symmetrical distribution with x axis. Combined with the stress distribution, the main cutting area can be defined for improving the machining efficiency to the local surface with high hardness.

Table 4 Binders for SCA

Group	1	2	3	4
Binder	Adhesive (706)	Epoxy (E44)	Epoxy (AB)	Acidic silicones

3. Experimental Procedures

3.1 Manufacture of SCA

In this study, the key point which needs to be figured out is that whether the abrasives can be uniformly consolidated on the surface of hemisphere rubber to achieve machining. Therefore, binder plays an important role in the manufacture of SCA.

In the process, the different kinds of binder were chosen for the manufacture as shown in Table 4. The carbofrax particles were adopted as abrasives.

For the purpose of stable machining of SCA, the followed important factors should be considered carefully in the process of manufacture, such as (1) Adhesive effect to the rubber; (2) Adhesive ability to the particle; (3) Wear resistance; (4) Thermal stability; (5) Moderate elasticity. Mark the layer of rubber matrix as the inner elastic layer and the layer of polymer binder as the outer elastic. The perfect effect of consolidation could result that the inner elastic medium has similar mechanical behavior with outer elastic medium. Interlayer between those double layers is in a complete continuous interface. Wang has presented combination conditions could be described as Eqs. (2) and (3).[19]

$$\begin{cases} \tau_{z1} = \tau_{z2} \\ \sigma_{z1} = \sigma_{z2} \end{cases} \quad (2)$$

$$\begin{cases} u_1 = u_2 \\ v_1 = v_2 \\ w_1 = w_2 \end{cases} \quad (3)$$

In Eqs. (2) and (3), τ_z is shear stress. σ_z is normal stress. u, v, w, are displacement on the direction of x, y, z, subscript 1 and 2 stand for the inner rubber layer and outer binder layer respectively. Therefore, the mechanical state of inner elastic layer is similar with the outer layers. The cutting stress of SAC exists in complex elastic medium and can be controlled by the inner air pressure expediently.

3.2 Machining experiment of SCA

The Motoman-HP20 with six degrees of freedom was utilized as robot arm whose location accuracy was 0.06 mm and load weight was 20 Kg.[20] It would be convenient when it machined with large freeform surface of the mold. The cutting area could reach at most 2.25 mm^2 (1.5 m × 1.5 m). The components of system were shown in Fig. 7.

Firstly, model of workpiece was established on the computer and trace of arm on the surface was auto-generated as program which was downloaded to the robot controller.

Secondly, the pneumatic wheel covered with SCA was equipped on

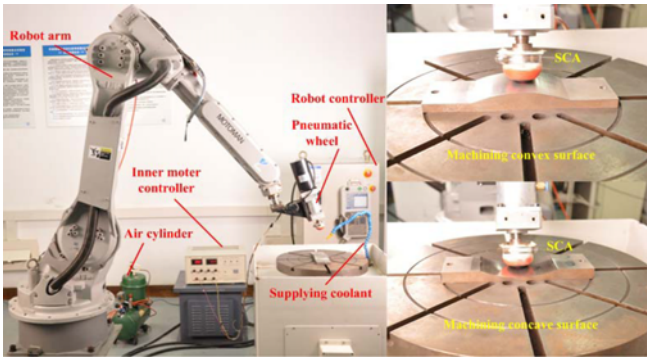

Fig. 7 Components of machining system

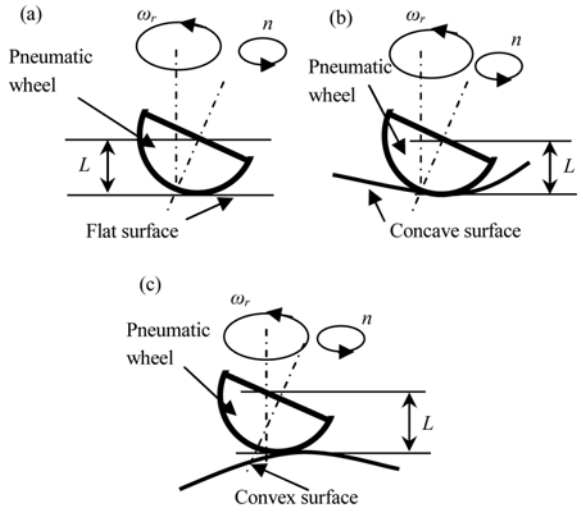

Fig. 8 Schematic diagram of pneumatic wheel: (a) Machining with flat surface, (b) Machining with concave surface, (c) Machining with convex surface

the robot arm and the air pressure is adjusted by the air cylinder. The rotation of wheel was controlled by inner motor.

Finally, the workpiece was fixed on the table and the pneumatic wheel began to machine. The gestures of pneumatic wheel were shown in Fig. 8. Where ω_r was angular velocity of wheel's revolution. It was mainly used to adjust the contact gesture between the wheel and workpiece for excellent cutting effect.

To complex freeform surface, the system could give full play to the advantages of robot-assisted to substitute ineffective manual way. Furthermore, the profiling ability of pneumatic wheel can compensate for the poor adaptability of rigid wheel machining.

The laser-quenching process to die steel was operated by the CO_2 laser system and the main factors of process were considered as Table 5. The level1's process stood for keeping original workpiece out of hardening. Level2's and level3's hardening process respectively improved hardness to 537 HV and 675 HV. The rest of constants in the workpiece went with Table 2.

The machining process had been divided into two stages as followed: (1) initial finishing and (2) precise polishing. Initial finishing process focused on high efficiency removal. R_a can be improved from 0.6~0.7 to 0.08~0.15 μm in a short time. Precise polishing process is

Table 5 Main factors considered in the laser hardening process

Factors	Level 1	Level 2	Level 3
Laser power	-	1500 W	1800 W
Energy density	-	15.83 J/mm^2	25 J/mm^2
Material	Cr12	Cr12	Cr12
Laser scanning speed	-	25 mm/s	12 mm/s
Laser spot size	-	4 mm	4 mm
Surface hardness	368 HV	537 HV	675 HV

Table 6 Parameters of machining

Initial average roughness of workpiece	0.653 μm
Feeding speed of wheel	660 mm/min
Processing time	100 s
Diameter of particle	96 μm

used to obtain mirror grade roughness improving R_a from 0.08~0.15 to 0.01 μm below. In this study, SCA mainly works on the initial finishing process aiming to achieve high efficiency to the freeform surface with high hardness.

For research on machining effects of SCA, the fixed machining experiments were carried out on the designated surface of workpiece, whose parameters were shown in Table 6. The carbofrax was adopted as abrasive particle. The rest of experimental parameters were in accordance with Table 3.

That SCA as a flexible body contacted with workpiece resulted in nonlinear stress in the contact process. However, it was found that Preston equation modified by recalculated stress could properly figure out this problem well, which was given as follows:[21]

$$M_r = K' P^{2/3} V \tag{4}$$

Where M_r standed for the material removal, P the stress, V the relative velocity, K' the constant. According to Figs. 4 and 6, the quality in the contact region would present difference. This point was investigated by the experiments.

At last, contrastive experiments were carried on respectively with SCA, freeform abrasives and fixed abrasives. Here, bonnet polishing method presented by Walker et al. was adopted as freeform abrasives machining because it was very close to the pneumatic wheel with SCA.[22] Besides, grinding wheel of fixed abrasives was manufactured with the same size as the bonnet and pneumatic wheel as mentioned by Jun et al.[23] The workpiece was in according with Table2's concave surface. Machining parameters were shown in Table 6. The surface micro results were shown by ZYGO.

4 Results and Discussions

4.1 Effects of consolidating abrasives

The pneumatic wheels with SCA had been manufactured by the contact laminating method with different binders as Table 4. The stability tests had been carried out for checking effects of consolidating abrasives. SCA underwent 30 min's machining process under the parameters in Table 3. The results were shown in Fig. 9.

It is found that a few abrasive particles have fallen down from the wheel when adhesive (706) is used as shown in Fig. 9(a). Fig. 9(b)

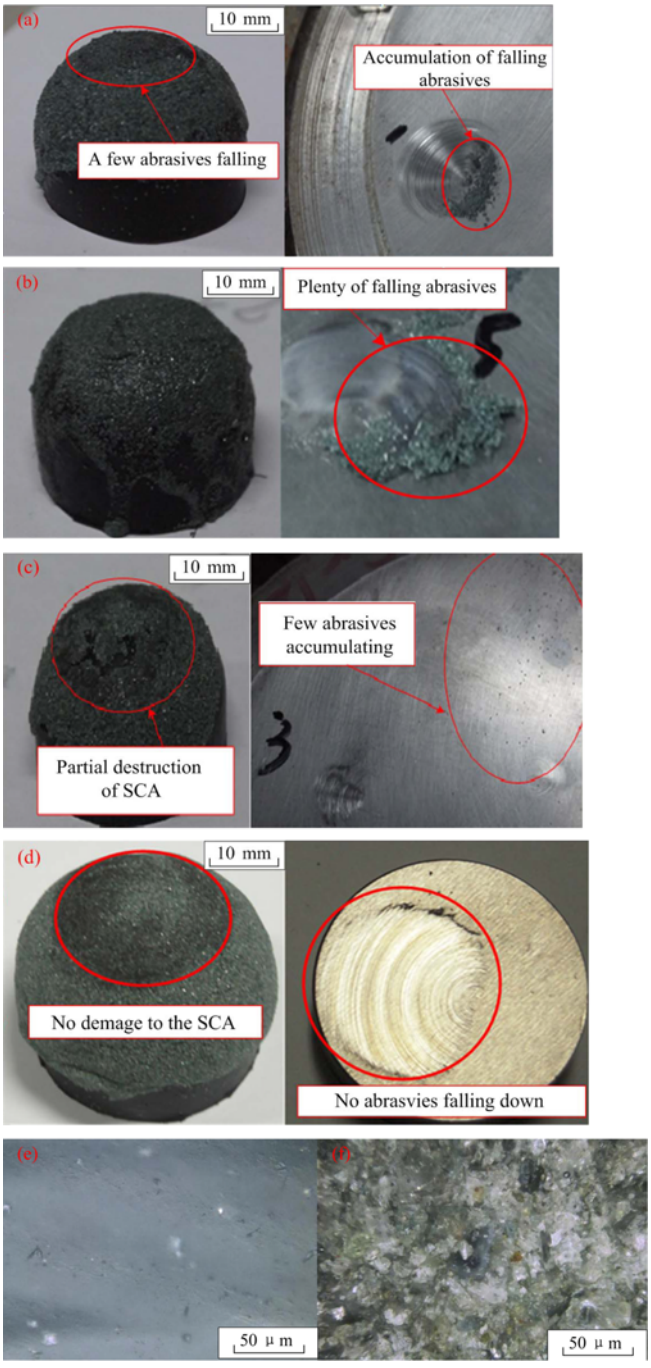

Fig. 9 Abrasives consolidating effects with kinds of binders as shows in (a)~(d): (a) Adhesive (706), (b) Epoxy (E44), (c) Epoxy(AB), (d) Acidic silicones, (e) Micrograph of binder, (f) Micrograph of SCA

shows epoxy (E44) leads to plenty of abrasive falling and accumulating on the workpiece. These mean that adhesive (706) and epoxy (E44) lack of the adhesion to the particles. Fig. 9(c) presents that epoxy (AB) holds abrasive particles on the outer layer of wheel, but produces partial destruction of SCA due to loss of adhesion to the inner hemisphere rubber layer of the wheel. Fig. 9(d) shows that acidic silicone has excellent effect of consolidating particles on the surface of wheel. Also there has not any destruction on SCA in the machining process. Fig. 9(e) takes on the microgram of SCA made by acidic silicone, which is obtained by the Keyence VK-9 700. In the situation of soft supporter,

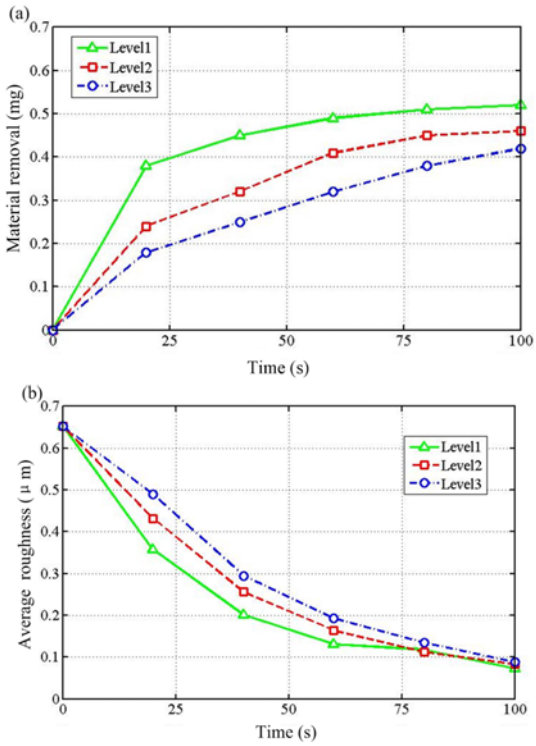

Fig. 10 Machining effects of SCA: (a) Material removal of SCA (b) Average roughness of workpiece

the micro-movement of abrasive particles will adjust the neighbor particle's cutting stress, which is in line with the analysis of Fig. 2.

4.2 Machining experiments of SCA

Fig. 10 shows the machining effects of SCA within a processing time of 100 seconds. The workpieces have been hardened according to the parameters shown in Table 5. The machining parameters are on the basis of Table 6.

The material removal had been recorded in Fig. 10(a). In the first 30 seconds, the material removal increases fast. During the period of dwell time from 30 to 60 s, the process of machining becomes tardy. Afterward, material removal varied slightly. Obviously, material removal to level1's workpiece is much higher than that to level2's and level3's, which is produced by the difference of hardness.

Fig. 10(b) shows profile average roughness in the processing time. After 100 s processing time there is an explicit improvement of average roughness. The quality is changing from $R_a = 0.653$ μm to $R_a = 0.08$ μm below. Longer processing time does not improve the surface quality anymore. In addition, the same processing quality to the level1~ level3's workpiece shows the final quality has little relationship with the hardness.

Fig. 11 shows the machining effect of SCA on the laser hardening surface. It is found that horniness is left by laser processing on the surface as Fig. 11(a) are cleaned out and altered into the slight scratches shown in Fig. 11(b) by SCA. The scratches always are in the same direction which causes the difference between horizontal roughness and vertical roughness.

The conclusion is that the surface hardness produced by the laser hardening process directly dominants the material removal, but has

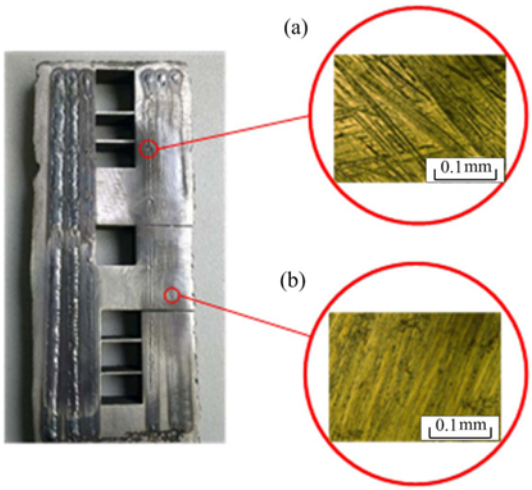

Fig. 11 Microgram of laser hardening surface: (a) Before machined (b) After machined by SCA

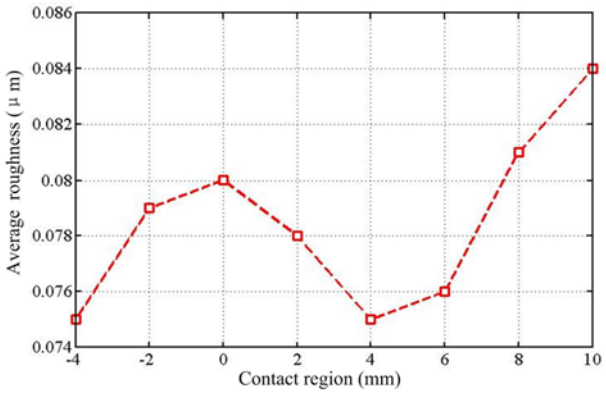

Fig. 12 Average roughness in the contact region

nothing to do with the final quality of surface. The average roughness (R_a = 0.08 μm below) finally obtained accords with the request of initial finishing process of SCA. Longer processing will not improve the quality of surface, but over cut and bring in damages to the surface. Furthermore, SCA needs to be adjusted by wheel's revolution (ω_r) all the time to avoid consistent scratches for improvement of quality.

The profile of average roughness in the contact region is illustrated in Fig. 12.

Where S = 0 mm is the center of contact region. It is found that R_a is almost symmetrically distributed with center point in the range of S from -4 to 4 mm. Afterward R_a increases with the S from 4 mm to the 10 mm. On the basis of Eq. (4), the trend of R_a accords with the distribution of stress in Fig. 4. And the max material removal region lies on the both neighbor sides of contact center. This characteristic can be used to machine the edges of hardening layer for weakening effect of different hardness.

4.3 Contrastive machining results and discussion

Fig. 13 shows the surface micro information including original surface and machining results.

Fig. 13(a) shows original surface where the horniness left by the

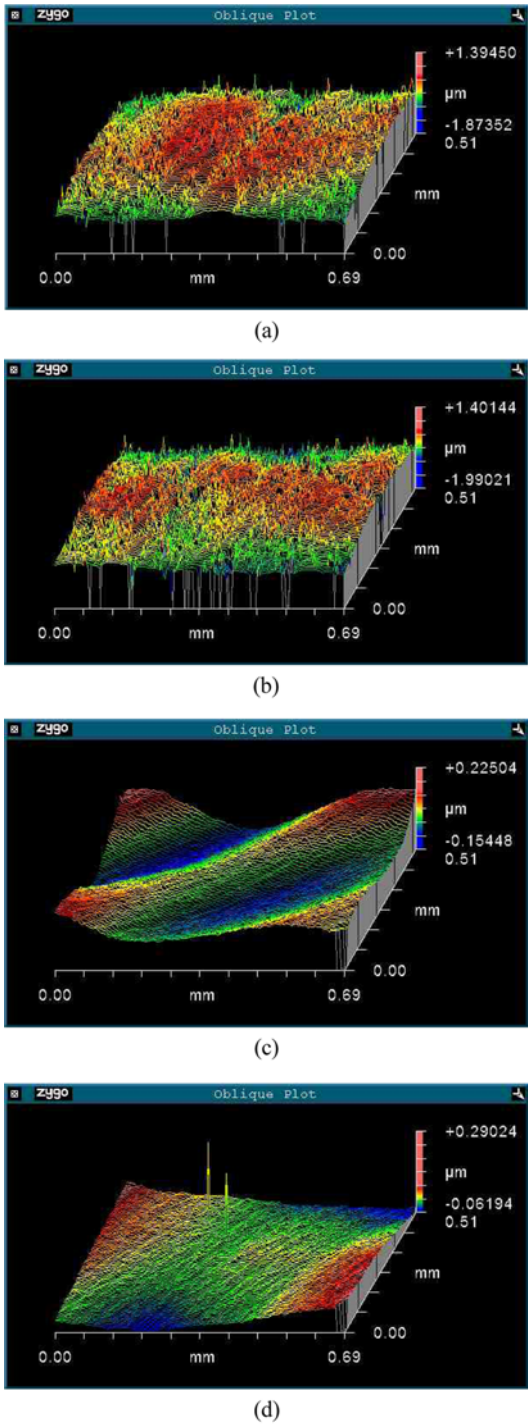

Fig. 13 Surface information: (a) Original surface, (b) Machining with freeform abrasives, (c) Machining with fixed abrasives, (d) Machining with SCA

laser processing exists. When it is machined by freeform abrasives, material is just removed only a little and surface quality is not improved as well, which is shown in Fig. 13(b). Though fixed abrasives lead to a large number of material removals, they cause the deep scratches on the curve surface as Fig. 13(c). However, SCA can improve the surface quality at the same time when it achieves material removal effectively as shown in Fig. 13(d).

The machining results above are in line with analysis of Fig. 2.

Freeform abrasives cannot supply enough cutting stress for the material removal when it faces with laser hardening surface. Fixed abrasives lack of self-adjusting ability in the contact process to fit for freeform surface and it results in deep scratches to weaken machining effects. Nevertheless, SCA method makes up for the two shortcomings above and has better machining effects than both of them.

5 Conclusions

(1) A new kind of finishing method based on SCA was brought forward for the laser hardening freeform surface. The abrasives were consolidated by the acidic silicone to constitute pneumatic wheel. Combined with robot, the system of machining had been established for dealing with the freeform surface.

(2) Though the laser hardening process increased the difficulty in finishing, SCA achieved explicit improvement of average roughness (R_a = 0.08 μm below) within 100 s, which accorded with the request of initial finishing process. For further improvement of average roughness, it was found that SCA needed to be adjusted by wheel's revolution (ω_r) all the time to avoid consistent scratches.

(3) Fig. 12 illustrated average roughness in the contact region. According to the Preston equation, combined with analysis of velocity, the trend of R_a matched with the distribution of stress in Fig. 4. This characteristic was fit for machining with the edges of hardening layer for weakening effect of different hardness.

(4) In the contrastive machining experiments among SCA, freeform abrasives and fixed abrasives, SCA machining method was confirmed to get higher material removal rate than free abrasive's and also possess better self-adjusting ability than fixed abrasives to fit for freeform surface. It has been an effective method for machining laser hardening freeform surface.

ACKNOWLEDGMENTS

This research is supported the National Natural Science Foundation of China (No. 51175471, No. 51405444) and Natural Science Foundation of Zhejiang Province (M503099). Industrial experiment is assisted by the financial support of Key Laboratory of Special Purpose Equipment and Advanced Manufacturing Technology Ministry of Education in Zhejiang University of Technology.

REFERENCES

1. Jeon, Y. and Lee, C. M., "Current Research Trend on Laser Assisted Machining," Int. J. Precis. Eng. Manuf., Vol. 13, No. 2, pp. 311-317, 2012.
2. Park, Y. J. and Lee, G. B., "Application of Heuristic Approaches to Minimization of Energy Consumption in Inner Layer Scrubbing Process in PCB Manufacturing," Int. J. Precis. Eng. Manuf., Vol. 13, No. 7, pp. 1059-1066, 2012.
3. Kennedy, E., Byrne, G., and Collins, D., "A Review of the Use of High Power Diode Lasers in Surface Hardening," Journal of Materials Processing Technology, Vol. 155-156, pp. 1855-1860, 2004.
4. Lamikiz, A., Sanchez, J., Lopez de Lacalle, L., and Arana, J., "Laser Polishing of Parts Built up by Selective Laser Sintering," International Journal of Machine Tools and Manufacture, Vol. 47, No. 12, pp. 2040-2050, 2007.
5. Ukar, E., Lamikiz, A., Lopez De Lacalle, L., Del Pozo, D., Liebana, F., and Sanchez, A., "Laser Polishing Parameter Optimisation on Selective Laser Sintered Parts," International Journal of Machining and Machinability of Materials, Vol. 8, No. 3, pp. 417-432, 2010.
6. Yasumaru, N., Sentoku, E., Miyazaki, K., and Kiuchi, J., "Femtosecond-Laser-Induced Nanostructure Formed on Nitrided Stainless Steel," Applied Surface Science, Vol. 264, No. pp. 611-615, 2013.
7. Yasa, E. and Kruth, J. P., "Investigation of Laser and Process Parameters for Selective Laser Erosion," Precision Engineering, Vol. 34, No. 1, pp. 101-112, 2010.
8. Yasa, E., Kruth, J. P., and Deckers, J., "Manufacturing by Combining Selective Laser Melting and Selective Laser Erosion/Laser Re-Melting," CIRP Annals-Manufacturing Technology, Vol. 60, No. 1, pp. 263-266, 2011.
9. Romoli, L., Tantussi, G., and Dini, G., "Layered Laser Vaporization of Pmma Manufacturing 3D MoUld Cavities," CIRP Annals-Manufacturing Technology, Vol. 56, No. 1, pp. 209-212, 2007.
10. Darafon, A., Warkentin, A., and Bauer, R., "3D Metal Removal Simulation to Determine Uncut Chip Thickness, Contact Length, and Surface Finish in Grinding," The International Journal of Advanced Manufacturing Technology, Vol. 66, No. 9-12, pp. 1715-1724, 2013.
11. Darafon, A., Warkentin, A., and Bauer, R., "Characterization of Grinding Wheel Topography using a White Chromatic Sensor," International Journal of Machine Tools and Manufacture, Vol. 70, No. pp. 22-31, 2013.
12. Mezghani, S. and El Mansori, M., "Abrasiveness Properties Assessment of Coated Abrasives for Precision Belt Grinding," Surface and Coatings Technology, Vol. 203, No. 5, pp. 786-789, 2008.
13. Huang, Y. and Huang, Z., "Development and Key Technologies of Abrasive Belt Grinding," Zhongguo Jixie Gongcheng/China Mechanical Engineering, Vol. 18, No. 18, pp. 2263-2267, 2007.
14. Tricard, M., Kordonski, W., Shorey, A., and Evans, C., "Magnetorheological Jet Finishing of Conformal, Freeform and Steep Concave Optics," CIRP Annals-Manufacturing Technology, Vol. 55, No. 1, pp. 309-312, 2006.
15. Ji, S., Li, C., Tan, D., Yuan, Q., Chi, Y., and Zhao, L., "Study on Machinability of Softness Abrasive Flow based on Preston Equation," Jixie Gongcheng Xuebao (Chinese Journal of Mechanical Engineering), Vol. 47, No. 17, pp. 156-163, 2011.

16. Smith, M., Guan, Z., and Cantwell, W., "Finite Element Modelling of the Compressive Response of Lattice Structures Manufactured using the Selective Laser Melting Technique," International Journal of Mechanical Sciences, Vol. 67, No. pp. 28-41, 2013.

17. Eriksen, R. S., Arentoft, M., Grønbæk, J., and Bay, N., "Manufacture of Functional Surfaces through Combined Application of Tool Manufacturing Processes and Robot Assisted Polishing," CIRP Annals-Manufacturing Technology, Vol. 61, No. 1, pp. 563-566, 2012.

18. Ji, S. M., Zeng, X., and Jing, M. S., "Soft-Consolidation Abrasives Pneumatic Wheel Technology Oriented to Finishing of High-Hardness Free-Form Surface," Key Engineering Materials, Vol. 523, No. pp. 149-154, 2012.

19. Wang, K., "Lay Elastic System Computer And Analysis," China Science Press, Chap. 4.3, 2009.

20. Ji, S. M., Jin, M. S., Zhang, X., Zhang, L., Zhang, Y. D., and Yuan, J. L., "Novel Gasbag Polishing Technique for Free-Form Mold," Chinese Journal of Mechanical Engineering, Vol. 43, pp. 2-6. 2007.

21. Zeng, X., Ji, S. M., Tan, D. P., Jin, M. S., Wen, D. H., and Zhang, L., "Softness Consolidation Abrasives Material Removal Characteristic Oriented to Laser Hardening Surface," The International Journal of Advanced Manufacturing Technology, Vol. 69, No. 9-12, pp. 2323-2332, 2013.

22. Walker, D. D., Beaucamp, A., Brooks, D., Freeman, R., King, A., et al., "Novel CNC Polishing Process for Control of Form and Texture on Aspheric Surfaces," Proc. of SPIE on Current Developments in Lens Design and Optical Engineering, Vol. 4767, pp. 99-105, 2002.

23. Qian, J., Li, W., and Ohmori, H., "Precision Internal Grinding with a Metal-Bonded Diamond Grinding Wheel," Journal of Materials Processing Technology, Vol. 105, No. 1, pp. 80-86, 2000.